HHS Public Access

Author manuscript

Nature. Author manuscript; available in PMC 2014 August 28.

Published in final edited form as:

Nature. 2013 May 2; 497(7447): 113–117. doi:10.1038/nature12063.

Random Convergence of Olfactory Inputs in the *Drosophila* Mushroom Body

Sophie J.C. Caron[1], **Vanessa Ruta**[2], **L. F. Abbott**[1,3], and **Richard Axel**[1,4,5]

[1] Department of Neuroscience, College of Physicians and Surgeons, Columbia University, New York, NY 10032, USA

[2] Laboratory of Neurophysiology and Behavior, The Rockefeller University, New York, NY, 10065, USA

[3] Department of Physiology and Cellular Biophysics, College of Physicians and Surgeons, Columbia University, New York, NY 10032, USA

[4] Department of Biochemistry and Molecular Biophysics, College of Physicians and Surgeons, Columbia University, New York, NY 10032, USA

[5] Howard Hughes Medical Institute

SUMMARY

The mushroom body (MB) in the fruit fly *Drosophila melanogaster* is an associative brain centre that translates odour representations into learned behavioural responses[1]. Kenyon cells (KCs), the intrinsic neurons of the MB, integrate input from olfactory glomeruli to encode odours as sparse distributed patterns of neural activity[2,3]. We have developed anatomic tracing techniques to identify the glomerular origin of the inputs that converge onto 200 individual KCs.

Here we show that each KC integrates input from a different and apparently random combination of glomeruli. The glomerular inputs to individual KCs exhibit no discernible organization with respect to their odour tuning, anatomic features, or developmental origins. Moreover, different classes of KCs do not appear to preferentially integrate inputs from specific combinations of glomeruli. This organization of glomerular connections to the MB could allow the fly to contextualize novel sensory experiences, a feature consistent with the role of this brain centre in mediating learned olfactory associations and behaviours.

Corresponding author Correspondence to: Richard Axel..

Contributions

S.J.C.C., V.R., L.F.A., and R.A. planned the research and wrote the paper; S.J.C.C. and V.R. performed the experiments; L.F.A. performed all statistical analyses.

SUPPLEMENTARY INFORMATION

Supplementary information is available in the online version of the paper at www.nature.com/nature.

Competing financial interests

The authors declare no competing financial interests.

Olfactory perception in the fly is initiated by the binding of an odorant to an ensemble of olfactory sensory neurons (OSNs) in the antennae, resulting in the activation of a unique and topographically fixed combination of glomeruli in the antennal lobe (AL)[2,3]. The discrimination of odours therefore requires the integration of information from multiple glomeruli in higher olfactory centres. AL projection neurons (PNs) extend dendrites into a single glomerulus and project axons that bifurcate to innervate two distinct brain regions, the lateral horn and the MB[4,5]. The invariant circuitry of the lateral horn is thought to mediate innate behaviours[6,7], whereas the MB translates olfactory sensory information into learned behavioural responses[1]. PN axons that innervate the MB terminate in large boutons[4,5] that synapse on KCs[6-8]. A given KC extends a small number of dendritic "claws", with each claw receiving information from only one PN bouton[8-10]. A single bouton connects to multiple KC claws to form a discrete anatomic structure, the microglomerulus[8-10]. Each KC projects an axon to one of the three different classes of MB lobes, α/β, α'/β', or γ, where it synapses upon a relatively small number of extrinsic output neurons[11,12].

Electrophysiological and optical imaging studies show that odorants activate sparse subpopulations of KCs[13] distributed across the MB without spatial preference[14]. Individual KCs could be connected to preferential combinations of glomeruli that are co-ordinately activated by behaviourally relevant odours. Alternatively, KCs may not receive structured input; rather the glomerular inputs may be random, a feature that maximizes the diversity of odour representations in the MB. We have exploited the specialized structure of the PN-KC synapse to characterize the glomerular origin of the PNs that converge onto individual KCs.

Photoactivatable green fluorescent protein (PA-GFP) was expressed in all neurons of the fly and a single KC was photolabelled. We observe that individual photolabelled KCs elaborate between 2 and 11 dendritic claws (average = 7, n = 200) restricted to the main olfactory calyx (Fig. 1b, h, Supplementary Table 1). The axonal projections of a labelled KC can be traced into either the α/β, α'β', or γ lobes of the MB (Fig. 1g, Supplementary Table 1). Texas red dextran was then electroporated into the centre of a single KC claw, filling the PN bouton innervating that claw (Fig. 1a-f). Retrograde transfer of the dye labels a single PN and its associated AL glomerulus (n = 665, Fig. 1g, Supplemental Table 1), providing further evidence that an individual KC claw receives input from only a single glomerulus.

We verified that this tracing method identifies functional connections between PNs and KCs. Functional imaging was performed on flies that express the calcium indicator GCaMP3 in most KCs to identify the claws activated by the stimulation of a single glomerulus (Fig. 2b). Electroporation of dye into an activated microglomerulus labels a single PN that innervates the stimulated glomerulus (n=10, Fig. 2c-f). Thus, the electroporation of dye into a KC claw allows us to faithfully identify the PN to which it is functionally connected.

We used the strategy of photolabelling a single KC and sequential electroporation of dye into each of its claws to define glomerular inputs to an individual KC. In initial experiments, PA-GFP was expressed in all neurons and 100 randomly chosen KCs were photolabelled in 100 different flies. Among the 100 photolabelled KCs, 84 α/β KCs, 14 α'/β' KCs, but only 2 γ KCs were identified (Supplementary Table 1). Each MB contains about 1000 α/β KCs,

370 α'β' KCs, and 670 γ KCs[15]. γKCs are underrepresented in this initial data set. This is likely to result from the spatial segregation of their cell bodies, which renders γ KCs less accessible to photolabelling. Most α/βKCs, but not the α/β and α'β' KCs, express Fruitless (Fru)[16-18]. An additional 100 γ KCs were targeted for photoactivation in flies expressing PA-GFP under the control of the Fru promoter (Supplementary Table 1).

Texas red dextran was sequentially electroporated into different claws of a photolabelled KC (Fig. 1h, i). It is technically difficult to fill all the claws of a KC and on average 3 glomerular inputs were identified per KC (Fig. 3, Supplementary Table 1). In fewer than 5% of the samples, the number of labelled PNs differed from the number of claws filled, reflecting either unsuccessful or imprecise electroporation. Samples with more labelled PNs than expected were discarded. The low frequency of unsuccessful claw fills indicates that claws extending from a given KC were filled with equal efficiency independent of size. Thus the size of a claw was not a selection criterion in these experiments.

A total of 683 inputs that synapse on 200 KCs were identified (Fig. 3, Supplemental Table 1). We found that 654 of these inputs connect to PNs innervating 49 of the 51 AL glomeruli. PNs innervating the DA3 and VL1 are absent from our data set but we observe boutons from these PNs in the MB calyx (Supplementary Fig. 1). 29 of the claws receive input from brain regions other than the AL. Interestingly, 11 of these claws are innervated by PNs that derive from pseudoglomeruli in the proximal antennal protocerebrum, a thermosensing centre in the fly brain that receives input from distinct heat- and cold-sensing neurons in the antennae[19]. The remaining 18 PNs innervated different uncharacterized regions of the brain.

We observe that the distribution of the glomerular inputs to KCs is not uniform (Fig. 3). Inputs from the DA1 and DC3 glomeruli are most frequent, with each accounting for 5.1% of the total connections. The non-uniform distribution reflects the fact that the size and number of calycal boutons formed by PNs varies across glomeruli (Supplementary Fig. 1). For instance, the PNs associated with the DA1 and DC3 glomeruli form more numerous boutons in comparison with the PNs of less frequently represented glomeruli (Supplementary Fig. 1). We also observe that there is a small but significant difference between the inputs to the α/β and γ KCs ($p < 0.001$) (Supplementary Fig. 2, 3). All subsequent statistical analyses were therefore performed separately on both the α/β and γ data sets, but failed to reveal any significant difference between the two data sets. Therefore, only the results obtained from the full data set are shown.

Statistical analyses of the 665 connections allow us to search for structure among the connections between glomeruli and KCs. First, we determined whether the KCs receiving input from a given glomerulus have a higher probability of receiving additional input from that same glomerulus. Of the 200 KCs in the data set, only 11 receive two inputs from the same glomerulus, and none receive three or more such inputs (Fig. 3, Fig. 4a, b). We determined whether the frequency of convergent input from a single glomerulus is significantly above or below chance expectations by randomly shuffling the connections in the data set between the different KCs, while maintaining the number of connections each of them receives. This shuffling maintains the frequency of glomerular connections observed in the experimental data, but eliminates any potential, non-random patterns of inputs onto

individual KCs. This shuffling is used in all subsequent statistical analyses. The frequency of multiple connections from the same glomerulus in the observed and shuffled data sets is not significantly different (Fig. 4b). Thus, we observe no KCs that receive preferential inputs from a single glomerulus. Rather, individual KCs integrate information from multiple different glomeruli.

We next determined whether KCs are connected to any preferential pair, trio, or quartet of glomeruli. Of the 1378 (53*52/2) different pairs of glomeruli that could converge onto an individual KC, 508 distinct pairs appear in the data set (Fig. 4a). 310 of these pairs connect to only one of the 200 KCs analysed, whereas certain pairs of glomeruli connect to multiple KCs (Fig. 4a, c). The DA1-DC3 pair, for example, converges onto nine different KCs (Fig. 3). There are combinations of glomerular trios that connect with two different KCs, and one case in which two KCs receive inputs from the same quartet of glomeruli (Fig. 3, Supplementary Table 1). However, the observed frequency with which the different pairs, trios and quartets converge onto different KCs is consistent with expectations from the shuffled data set (Fig. 4c, data not shown). Thus, the identity of a glomerulus connected to a KC provides no predictive information as to the identity of the remaining glomerular inputs onto that neuron.

Glomeruli can be grouped based on biological properties shared by their associated OSNs (sensilla type, odour specificity) and PNs (developmental origin and topography of their axonal projections). KCs might receive preferential input from one or another of these glomerular categories. For example, the OSNs innervating the AL are derived from three sensillar types (basiconic, coeloconic, and trichoid sensilla) that project to three classes of glomeruli tuned to different odour categories[20]. If individual KCs were tuned to a particular class of odours, they might preferentially integrate inputs from one type of sensillum. Statistical analyses, however, reveal that KCs that receive an input from one sensillar type are no more or less likely to receive additional inputs from this or any other type of sensillum than is predicted by chance (Fig. 4e-h). Sensillar type, however, provides only a coarse correlate of odour tuning. Therefore, we also grouped glomeruli based on the similarity of their odour response profiles and again observed no structure in the inputs to a KC that correlated with odour tuning (Supplementary Fig. 4).

We also classified glomeruli on the basis of the properties of their PNs. PN axons from different glomeruli project to broad but stereotyped domains in the lateral horn and calyx of the MB. Input to an individual KC could be shaped by the topography of PN projections. Analysis of the distribution of inputs to a given KC, however, fails to reveal any preferential PN connectivity that reflects the organization of their projection[7] in either the MB calyx (Fig. 4d, Supplementary Fig. 5) or lateral horn (Fig. 4d, Supplementary Fig. 6). KCs do not preferentially integrate information from glomeruli innervated by PNs sharing a developmental origin[21] (Fig. 4d, Supplementary Fig. 7). In addition, KCs do not select their input based on topographical constraints as suggested by a previous study[22] (Fig 4d, Supplementary Fig. 8). Finally, three glomeruli are innervated by Fru-expressing OSNs and PNs[16,17]. We do not observe preferential pairing of inputs from Fru^+ PNs onto individual KCs (Fig. 4d, Supplementary Fig. 9). Moreover, although most γ KCs express Fru, there is no preferential input from Fru^+ glomeruli to γ KCs (Supplementary Fig. 2).

Next, we performed an unbiased search for structure by examining correlations within the connectivity matrix between the 53 glomeruli (51 AL glomeruli and 2 pseudoglomeruli) and the 200 KCs. Correlations were extracted by performing a principal component analysis of this matrix (Supplementary Fig. 10, 11). This analysis failed to reveal structure in the input to KCs other than that inherent in the non-uniform distribution of glomerular inputs.

These data are consistent with a model in which each KC receives input from a combination of glomeruli randomly chosen from the non-uniform distribution of glomerular projections to the MB. Classification of either glomeruli or KCs on the basis of several shared developmental, anatomic, and functional features fails to reveal structured input onto individual KCs. Members of a given PN class do not preferentially converge onto an individual KC nor do members of a KC class receive specific and distinguishing PN inputs. A given KC can integrate information from glomeruli activated by food odours, pheromones, CO_2 and even temperature. Recent data suggests that the extrinsic output neurons of the MB that are responsible for the different forms of learned behaviour are anatomically segregated and synapse with KC axons within a specific MB lobe[12,18]. Interestingly, similar glomerular inputs are observed for the KCs that innervate the different lobes of the MB. This random input to individual KCs provides a mechanism to contextualize a rich diversity of novel KC responses.

It is important to note that the tracing procedure we have developed only allows us to characterize the inputs to a single KC per fly. It is therefore possible that the inputs to every KC are determined but this developmental program results in a distribution of glomerular inputs that appears random. However, it is difficult to conceive of a development mechanism that could dictate the identity of inputs to each of the seven claws of the 2000 KCs. Moreover, the logic of employing complex and unlikely identity codes to achieve an uncorrelated distribution of inputs is elusive. Indeed, a previous study examined the electrophysiological response of KCs to different odours in a line of flies that labels only 23 α/β neurons but failed to identify replicate KCs with shared odour response profiles[23]. These observations support the conclusion that the complement of glomerular inputs to KCs differs in different individuals. In addition, we cannot, from the analysis of the glomerular inputs to 200 KCs, exclude the existence of small subsets of KCs that received determined inputs from the AL. Nonetheless, our data are most consistent with a model in which the majority of individual KCs receive input from a random collection of glomeruli, a finding with important implications for odour processing in the MB.

If the connections from AL to MB are indeed random, a given odour will activate a different ensemble of KCs in different flies. However, in an individual fly, a given odour will consistently activate the same ensemble. This representation must acquire valence through experience or unsupervised activity dependent plasticity to dictate an appropriate behavioural output. Uncorrelated glomerular input to KCs affords the fly with the ability to impart meaning to a diversity of novel and unpredictable sensory stimuli that it may encounter throughout its life. Plasticity at highly convergent synapses between KC axons and MB extrinsic neurons could mediate experience-dependent behavioural output, an elemental feature of MB function. Thus, the fly has evolved an olfactory circuit with a

connectivity that optimizes its ability to contextualize and respond appropriately to a rich array of olfactory experiences.

METHODS

Fly stocks

All fly transgenic lines (synaptobrevin^{GAL4}, OK107^{GAL4}, GH146^{GAL4}, Fruitless^{GAL4}, UAS-C3PA-GFP, UAS-SPA-GFP, and UAS-GCaMP3) have been described previously[25-28].

Imaging

All imaging experiments were performed using an Ultima two-photon laser scanning microscope (Prairie Technologies) equipped with galvonometers driving a Chameleon XR laser (Coherent). Emitted photons were collected with a GaAsP photodiode detector (Hamamatsu) or a PMT detector through a 60X 0.9 N.A. water immersion objective (Olympus). All images were acquired at a resolution of 512 by 512 pixels using 1 μm intervals between optical slices.

Photolabelling neurons through photoactivation of PA-GFP

Individual neurons were photolabelled by converting PA-GFP under the guidance of a two-photon microscope. In an initial set of experiments, individual KC soma were randomly selected for photolabelling in flies expressing one copy of UAS-SPA and two copies of UAS-C3PA[25] under the control of the pan-neuronal promoter synaptobrevin^{GAL4}. The number of γ KCs labelled using this procedure was lower than expected. This most likely reflects the fact that the somas of these neurons are buried at the core of the MB, a region less accessible to photoactivation. We therefore corrected for this bias by generating a second set of experiments using a γ KCs specific promoter. In this set, individual γ KCs were photolabelled in flies expressing two copies of UAS-C3PA under the control of the Fruitless^{GAL4}. In this set of experiments, flies also expressed C3PA-GFP in the majority of the PNs using the GH146^{GAL4} promoter to facilitate the identification of dye-labeled glomeruli in the AL. In all experiments, the brains of 1-3 days old male flies isolated from females after eclosion were dissected in saline (108 mM NaCl, 5 mM KCl, 2 mM $CaCl_2$, 8.2 mM $MgCl_2$, 4 mM $NaHCO_3$, 1 mM NaH_2PO_4, 5 mM trehalose, 10 mM sucrose, 5 mM HEPES, pH 7.5, osmolarity adjusted to 275 mOsm) and incubated in 2 mg/mL collagenase (Sigma-Aldrich) for approximately 1 minute. Brains were pinned on a thin sheet of Sylgard (World Precision Instruments) placed at the bottom of an imaging chamber filled with saline. The MB was first imaged at 925 nm (a wavelength at which photoconversion is relatively inefficient) in order to define a region of interest over the soma of the targeted KC. PA-GFP was subsequently photoactivated within that region through consecutive exposures to 710 nm laser light (a wavelength that efficiently photoconverts the fluorophore). A resting period of 10 minutes was allowed for the photoconverted fluorophore to diffuse into the distal KC processes. Photoactivation power was typically between 9 and 30 mW measured at the back of the objective and exposure time was less than 1 s. KCs that extend dendritic claws only to the accessory calyx but not the main olfactory calyx were found but these KCs were not used in this study. All the PNs innervating a particular glomerulus were

photolabelled in flies expressing one copy of UAS-SPA and two copies of UAS-C3PA under the control of the panneuronal driver synaptobrevin^{GAL4} using a similar strategy (photoactivation power: between 25 and 32 mW, photoactivation exposure time: on average 1 minute, resting time: 30 minutes).

Electroporation of dye into the PN connected to a KC claw

The PNs connected to a given photolabelled KC were identified by sequentially electroporating 100 mg/mL 3,000-Da Texas-red dextran dye (Invitrogen) into individual KC claws. Glass electrodes (Sutter Instruments) were pulled to a resistance of 9-11 MΩ. Each electrode was fire-polished using a micro-forge (Narishige) to narrow its opening. Electrodes were back-filled with the dye. Under the guidance of a two-photon microscope, the electrode was centred into a photolabelled KC claw using motorized manipulators (Sutter Instruments). Short current pulses (each 30-50 V for 0.5 ms) were used to electroporate the dye into the PN bouton connected to the targeted claw. Although small claws are as easy to fill as larger ones, filling all the claws formed by a given KC was technically challenging because the photolabel weakens as more electroporations are performed on the same neuron. In less than 5% of experiments, the number of labelled PNs was larger than the number of claws filled and these samples were discarded. A smaller number of samples had fewer labelled PNs than expected, most likely because one or more of the labelled claw(s) were not properly filled. A z-stack of the entire AL was taken at the end of the experiment. Dye-labelled glomeruli were identified using the basal fluorescence of PA-GFP expressed in all or most PNs (under the control of the pan-neuronal promoter synaptobrevin or the PN specific GH146 promoter). Dye-labelled glomeruli were identified on the basis of their stereotyped position and shape in the AL, as well as the location of the soma of their associated PNs and whether they were GH146+. The glomeruli connected to each of the 200 KCs were analysed by the same person. First, the 654 labelled glomeruli were identified in the 200 AL. This identification was repeated without consideration to the previous designation and the mismatch rate between the two scores was determined. This procedure was repeated until the mismatch rate was lower than 5% (about 15 rounds). This approach permitted the observer to become extremely familiar with characteristic properties of the glomerular map in the AL so that the mismatch rate diminished considerably in later rounds. In addition, the same identified glomeruli were compared across samples to ascertain that a given glomerulus displays the same shape and general location in all ALs. Although we cannot exclude that some glomeruli might have been misidentified, such error will most likely be consistent across the data set and thus should not alter the conclusion of our study.

Functional imaging

Optical imaging experiments were performed in flies expressing two copies of UAS-GCaMP3 under the control of the KC specific OK107^{GAL4} promoter. The brains of 1-2 days old male flies were dissected, desheathed, and pinned on a thin sheet of Sylgard in an imaging chamber filled with saline. Single glomeruli were stimulated as previously described[25]. In summary, glass electrodes were pulled to a resistance of 7–8 MΩ and filled with 2 mM acetylcholine (Sigma-Aldrich). 3,000 Da Alexa-488 dextran was added at 0.5 mg/mL to the acetylcholine to allow for fluorescent visualization of the stimulating

electrode. The stimulating electrode was positioned into the centre of a superficial glomerulus and short current pulses (each 0.5-2V for 500 ms) generated by a stimulator (Grass Technologies) allowed for selective and synchronous stimulation of the PNs innervating the impaled glomerulus. Images of the MB calyx were acquired at 925 nm at a frequency of 2 Hz. Activated KC claws within an individual microglomeruli displayed increases in fluorescence and were targeted with a glass electrode filled with Texas-red dye. Electroporation of the dye into the activated microglomerulus was performed as described in the previous section.

Image processing

Maximum-intensity projections of z-stacks were generated in ImageJ (NIH). In some experiments (e.g. Figure 1g), out of plane fluorescence at the surface of the brain arising from auto-fluorescence of the glial sheath was masked.

Statistical analyses

All experimentally derived results were compared with those obtained from 1000 shuffled data sets. We generated the shuffled data by making a list of the glomeruli that contributed to the 665 connections in the data. We then randomly permuted this list and drew from it sequentially to construct a new set of connections for 200 model KCs, drawing as many random connections for each model KC as it receives in the experimental data. This shuffling maintains the frequency of glomerular connections and the number of connections per KC observed in the experimental data, but eliminates any potential, non-random patterns of inputs onto individual KCs.

Distribution of the glomerular inputs: The uniformity of the distribution of the 665 experimentally derived connections between glomeruli and KCs was quantified for the full data set as well as for different KC subpopulations using a Xi-squared measure.

Pairwise analysis: The frequency of a KC receiving two inputs from a given pair of glomeruli was measured for all 1378 different possible pairs (51 AL glomeruli and 2 thermosensing pseudo glomeruli). Pairwise analysis was performed on both the experimentally derived and shuffled data sets.

Group analyses: The 51 AL glomeruli were grouped according to different criteria (the two thermosensing pseudo glomeruli were grouped as “other” for these analyses). For each criterion, the distribution of the 665 experimentally derived connections was determined across all groups. KCs with at least one connection to a particular group were selected and the distribution of their remaining inputs was compared to that of the full data set. We performed similar analyses on the shuffled data. The distributions obtained from the experimental and shuffled data sets were compared to search for any positive or negative correlations that were statistically significant. This analysis examines whether the probability of a KC receiving a connection from a glomerulus of type A, P(A), is equal to the conditional probability P(A|B), conditioned on its receiving one input from a glomerulus of type B. The following criteria were tested:

Type of sensillum—Glomeruli were clustered into three groups based on their sensillar origin[20].

Odour response profile—Glomeruli were clustered into three groups based on the similarity of the odour response profiles of their associated OSNs as measured in a previous study[24].

PN overlap (calyx)—Glomeruli were clustered into four groups based on the overlap of their associated PNs in the calyx of the MB as measured in a previous study[7].

PN overlap (lateral horn)—Glomeruli were clustered into five groups based on the overlap of their associated PNs in the lateral horn as measured in a previous study[7].

Zonal overlap—Glomeruli were clustered into five groups as defined by a previous study that found correlations in the topography of PN boutons and KC dendrites in the MB calyx[22].

PN lineage—Glomeruli were clustered into three groups based on the developmental origin of their associated PNs as determined in a previous study[21].

Fru expression—Glomeruli were clustered into two groups given that their associated OSNs and PNs both express (or not) Fru[16,17].

Singular value decomposition—Singular value decomposition was performed on the experimentally derived connectivity matrix as well as on the shuffled data to test for statistical significance. Any matrix can be expressed as the product of an orthogonal matrix, a diagonal matrix, and another orthogonal matrix in what is called a singular value decomposition. Large singular values, the non-zero elements of the diagonal matrix, correspond to structure detected in the original matrix. The corresponding rows or columns of the orthogonal matrices provide projections reflecting this structure. Examples of the sensitivity of this method for revealing structure in connectivity matrices are shown in Supplementary Fig. 11. The percent variances reported are the squares of the singular values.

Supplementary Material

Refer to Web version on PubMed Central for supplementary material.

ACKNOWLEDGMENTS

We thank Cori Bargmann, Tom Jessell, Florian Maderspacher, Liam Paninski and members of the Axel lab for comments on the manuscript; Cynthia Franqui for assistance with fly work; and Phyllis Kisloff, Miriam Gutierrez, and Adriana Nemes for assistance with general laboratory concerns and the preparation of this manuscript. This work was funded in part by a grant from the Foundation for the National Institutes of Health through the Grand Challenges in Global Health Initiative (RA). Further financial support was provided by the Howard Hughes Medical Institute (RA), by the Swartz and Gatsby Foundations (LFA) and by the Pew Charitable Trusts, McKnight Foundation, and New York Stem Cell Foundation (VR).

REFERENCES

1. Heisenberg M. Mushroom body memoir: from maps to models. Nat Rev Neurosci. 2003; 4:266–275. [PubMed: 12671643]
2. Wang JW, Wong AM, Flores J, Vosshall LB, Axel R. Two-photon calcium imaging reveals an odor-evoked map of activity in the fly brain. Cell. 2003; 112:271–282. [PubMed: 12553914]
3. Ng M, et al. Transmission of olfactory information between three populations of neurons in the antennal lobe of the fly. Neuron. 2002; 36:463–474. [PubMed: 12408848]
4. Wong AM, Wang JW, Axel R. Spatial representation of the glomerular map in the Drosophila protocerebrum. Cell. 2002; 109:229–241. [PubMed: 12007409]
5. Marin EC, Jefferis GS, Komiyama T, Zhu H, Luo L. Representation of the glomerular olfactory map in the Drosophila brain. Cell. 2002; 109:243–255. [PubMed: 12007410]
6. de Belle JS, Heisenberg M. Associative odor learning in Drosophila abolished by chemical ablation of mushroom bodies. Science. 1994; 263:692–695. [PubMed: 8303280]
7. Jefferis GS, et al. Comprehensive maps of Drosophila higher olfactory centers: spatially segregated fruit and pheromone representation. Cell. 2007; 128:1187–1203. [PubMed: 17382886]
8. Butcher NJ, Friedrich AB, Lu Z, Tanimoto H, Meinertzhagen IA. Different classes of input and output neurons reveal new features in microglomeruli of the adult Drosophila mushroom body calyx. J Comp Neurol. 2012; 520:2185–2201. [PubMed: 22237598]
9. Leiss F, Groh C, Butcher NJ, Meinertzhagen IA, Tavosanis G. Synaptic organization in the adult Drosophila mushroom body calyx. J Comp Neurol. 2009; 517:808–824. [PubMed: 19844895]
10. Yasuyama K, Meinertzhagen IA, Schurmann FW. Synaptic organization of the mushroom body calyx in Drosophila melanogaster. J Comp Neurol. 2002; 445:211–226. [PubMed: 11920702]
11. Tanaka NK, Tanimoto H, Ito K. Neuronal assemblies of the Drosophila mushroom body. J Comp Neurol. 2008; 508:711–755. [PubMed: 18395827]
12. Sejourne J, et al. Mushroom body efferent neurons responsible for aversive olfactory memory retrieval in Drosophila. Nat Neurosci. 2011; 14:903–910. [PubMed: 21685917]
13. Turner GC, Bazhenov M, Laurent G. Olfactory representations by Drosophila mushroom body neurons. J Neurophysiol. 2008; 99:734–746. [PubMed: 18094099]
14. Honegger KS, Campbell RA, Turner GC. Cellular-resolution population imaging reveals robust sparse coding in the Drosophila mushroom body. J Neurosci. 2011; 31:11772–11785. [PubMed: 21849538]
15. Aso Y, et al. The Mushroom Body of Adult Drosophila Characterized by GAL4 Drivers. J Neurogenet. 2009:1–17.
16. Manoli DS, et al. Male-specific fruitless specifies the neural substrates of Drosophila courtship behaviour. Nature. 2005; 436:395–400. [PubMed: 15959468]
17. Stockinger P, Kvitsiani D, Rotkopf S, Tirian L, Dickson BJ. Neural circuitry that governs Drosophila male courtship behavior. Cell. 2005; 121:795–807. [PubMed: 15935765]
18. Keleman K, et al. Dopamine neurons modulate pheromone responses in Drosophila courtship learning. Nature. 2012
19. Gallio M, Ofstad TA, Macpherson LJ, Wang JW, Zuker CS. The coding of temperature in the Drosophila brain. Cell. 2011; 144:614–624. [PubMed: 21335241]
20. Vosshall LB, Stocker RF. Molecular architecture of smell and taste in Drosophila. Annu Rev Neurosci. 2007; 30:505–533. [PubMed: 17506643]
21. Yu HH, et al. A complete developmental sequence of a Drosophila neuronal lineage as revealed by twin-spot MARCM. PLoS Biol. 2010:8.
22. Lin HH, Lai JS, Chin AL, Chen YC, Chiang AS. A map of olfactory representation in the Drosophila mushroom body. Cell. 2007; 128:1205–1217. [PubMed: 17382887]
23. Murthy M, Fiete I, Laurent G. Testing odor response stereotypy in the Drosophila mushroom body. Neuron. 2008; 59:1009–1023. [PubMed: 18817738]
24. Hallem EA, Carlson JR. Coding of odors by a receptor repertoire. Cell. 2006; 125:143–160. [PubMed: 16615896]

25. Ruta V, et al. A dimorphic pheromone circuit in Drosophila from sensory input to descending output. Nature. 2010; 468:686–690. [PubMed: 21124455]

26. Pauli A, et al. Cell-type-specific TEV protease cleavage reveals cohesin functions in Drosophila neurons. Dev Cell. 2008; 14:239–251. [PubMed: 18267092]

27. Connolly JB, et al. Associative learning disrupted by impaired Gs signaling in Drosophila mushroom bodies. Science. 1996; 274:2104–2107. [PubMed: 8953046]

28. Stocker RF, Heimbeck G, Gendre N, de Belle JS. Neuroblast ablation in Drosophila P[GAL4] lines reveals origins of olfactory interneurons. J Neurobiol. 1997; 32:443–456. [PubMed: 9110257]

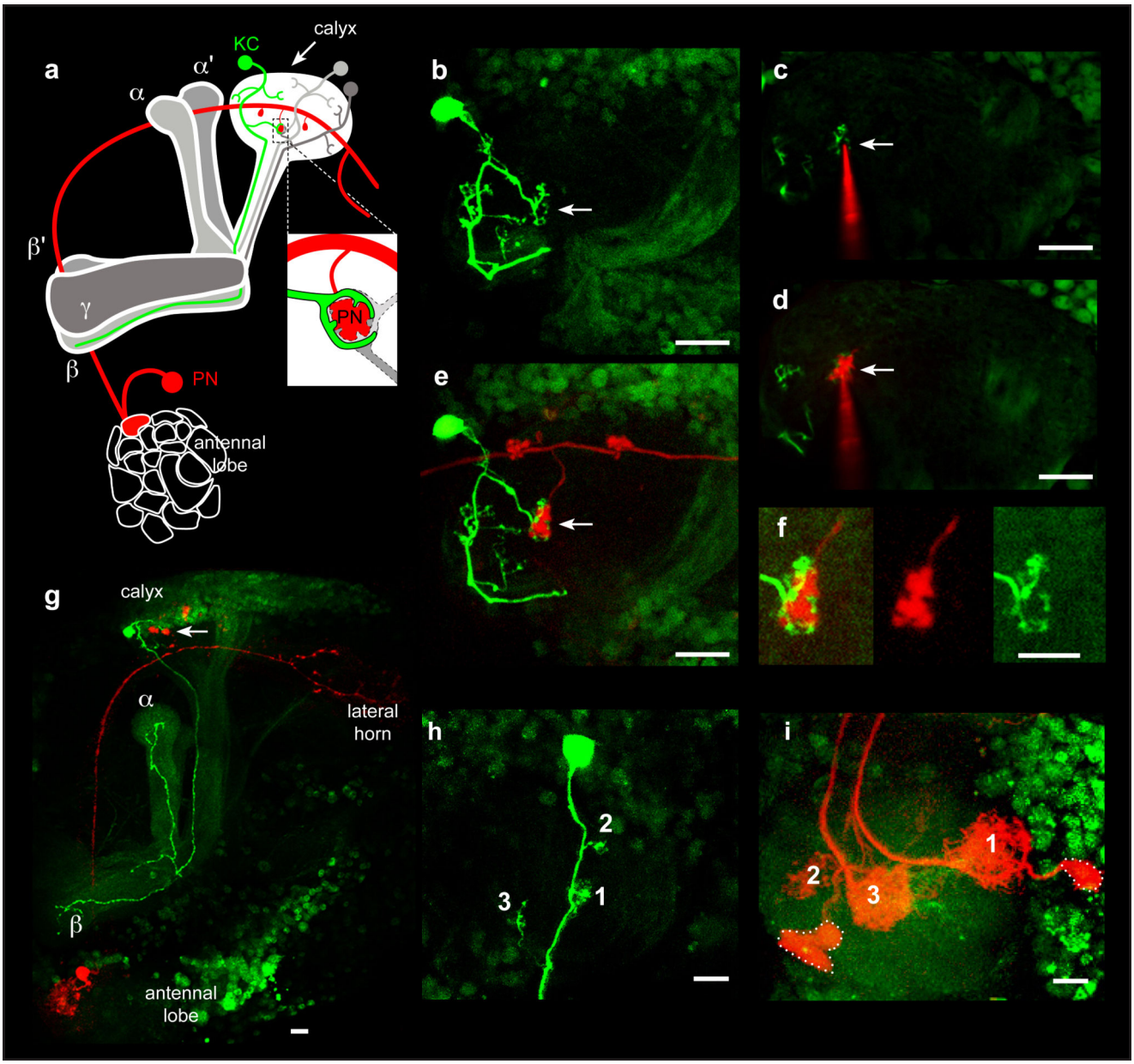

Figure 1. Dye-electroporation labels the PN connected to a KC claw

a Schematic illustration of the tracing strategy used to identify the PN connected to a single KC claw. PNs (one shown in red) transmit olfactory information from a single glomerulus in the AL to the MB by forming multiple axonal boutons in the calyx. KCs extend dendrites into the MB calyx (white) and project axons into either the α/β (light gray), α'/β' (medium gray), or γ (dark gray) lobe. The microglomerulus highlighted by a single photolabelled KC (green) is targeted for electroporation of red dye, resulting in the uptake of dye by a single PN and its associated AL glomerulus (red). Insert shows the targeted microglomerulus formed from a singe red PN bouton connected to the photolabelled KC claw (green) as well as other unlabeled KC claws (different shades of gray). **b**, Photolabelling of a single KC expressing PA-GFP under the control of the panneuronal promoter synaptobrevin^{GAL4}

reveals 6 dendritic claws within the MB calyx. **c**, An electrode filled with Texas Red dextran is centered into the microglomerulus outlined by one of the photolabelled KC claws shown in **b** (arrow). **d**, Dye is electroporated into the targeted microglomerulus (arrow). **e**, Electroporated dye labels a single PN (n=684), which has a bouton that innervates the targeted microglomerulus (arrow). Note that the other KCs that synapse on this PN bouton were not labeled in this example. **f**, The photolabelled claw ensheathes the red dye-labeled PN bouton. Scale bar, 5 microns. **g**, The photolabelled KC projects to the α/β lobes of the MB whereas the dye-labeled PN it innervates the DM6 glomerulus **h**, A photolabelled KC with 3 claws. **i**, Three PNs innervating the DA1, VC4, and DL3 glomeruli are labeled upon loading all the claws of the KC depicted in **h.**Soma of the DA1 PN and VC4 PN are outlined while the DL3 soma is out of the plane. All scale bars are 10 microns except where noted.

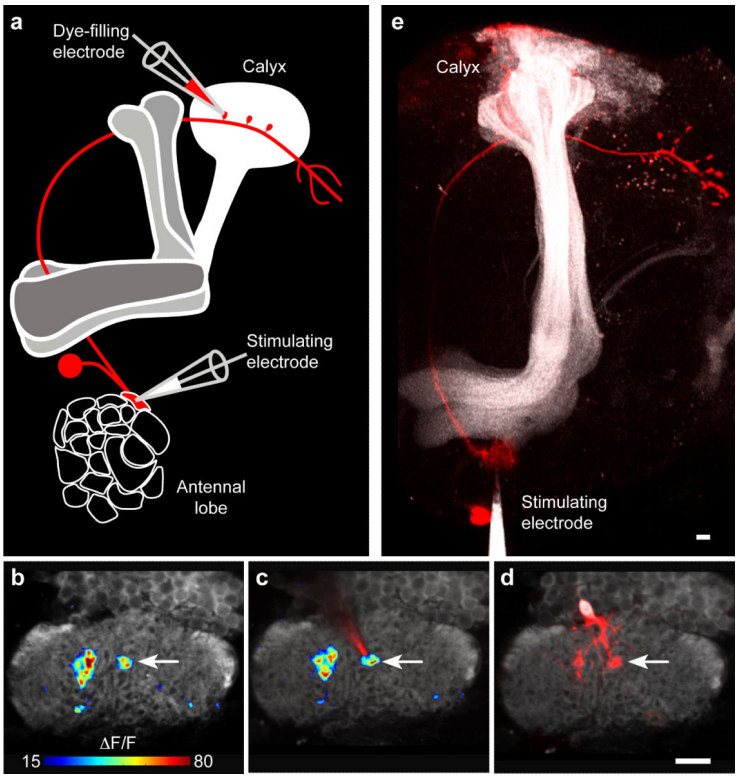

Figure 2. Dye-labeling identifies functional connections between PNs and KCs

a Schematic illustration of the strategy used to identify functional connections between PNs and KCs. An AL glomerulus (here DL3) is stimulated by local iontophoresis of acetylcholine (stimulating electrode). Optical recordings of calcium-mediated changes in fluorescence (ΔF/F) are measured in the MB calyx of a fly expressing GCaMP3 driven by the KC specific promoter $OK107^{GAL4}$. A microglomerulus activated by the stimulation of DL3 is targeted for dye electroporation, identifying the pre-synaptic PN (red). **b**, Stimulation of the DL3 glomerulus activates several microglomeruli dispersed through the calyx. **c**, An electrode filled with Texas Red dextran is positioned into the center of an activated microglomerulus (arrow) highlighted by the recorded ΔF/F. **d**, Electroporation of dye into the targeted microglomerulus labels a single PN bouton (arrow). **e**, The labeled bouton extends from a single dye-filled PN that innervates the stimulated DL3 glomerulus (n=10). Note that the stimulating electrode is visualized by addition of Alexa-488 dextran dye to the acetylcholine. Scale bars are 10 microns.

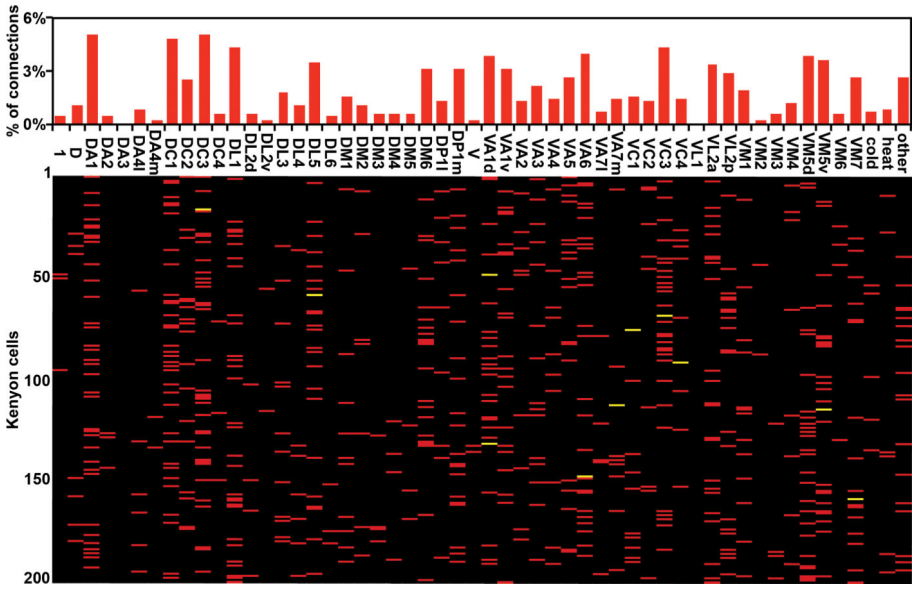

Figure 3. The connectivity matrix between AL glomeruli and KCs

The 665 connections between the AL glomeruli and KCs are represented in a matrix in the lower panel. Each row corresponds to one of the 200 photolabelled KCs while each column refers to the 51 AL glomeruli, the 2 thermo-sensing pseudoglomeruli and the other uncharacterized brain regions. Glomeruli connected once to a given KC are depicted as red bars. Glomeruli connected twice to the same KC are labeled as yellow bars. In the upper panel, the connections to all glomeruli and other brain regions are sorted according to their observed frequency.

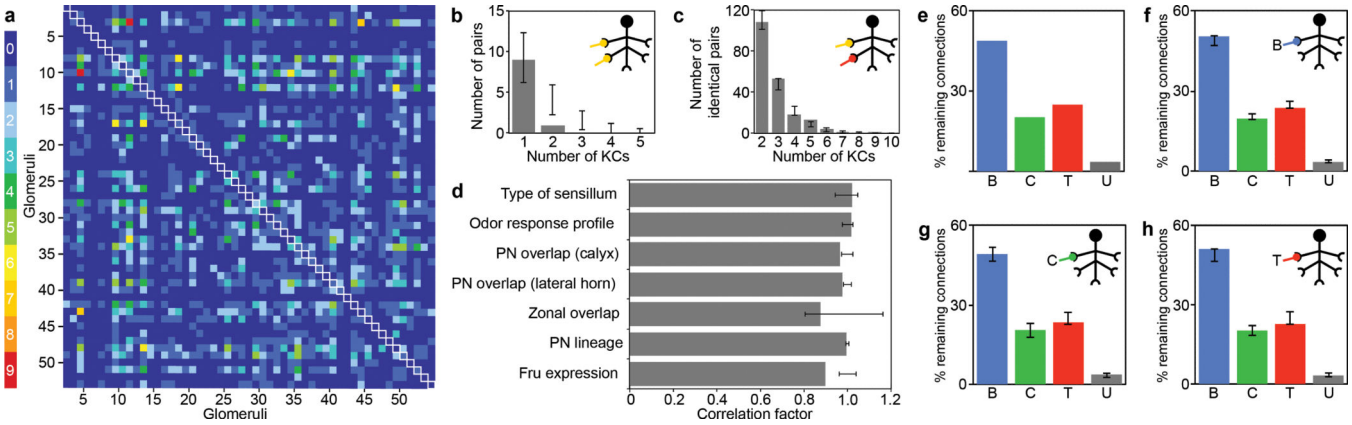

Figure 4. KCs do not receive structured input

a Two glomeruli projecting to the same KC are considered a connected pair. All possible pairs of glomeruli are depicted as squares in a 53 x 53 matrix (51 AL glomeruli and 2 pseudoglomeruli), colored according to their observed frequency in the data (white outlined squares along the diagonal depict the frequency of identical pairs where a glomerulus is paired with itself). **b**, The frequency of KCs receiving two connections from the same glomerulus (an identical pair, gray bars) is compared to the frequency of such cells in 1,000 shuffled data sets (black circles: average, error bars: ± s.d.). **c**, The frequency of KCs receiving input from the same non-identical pair (gray bars) is compared to the frequency of such cells in 1,000 shuffled data sets (black circles: average, error bars: ± s.d.). **d**, Glomeruli are grouped based upon different anatomic or functional parameters[7,17,20-22,24]. For each listed parameter, the percentage of connections across KCs receiving at least one input from a given group (as shown in **f**, **g**, and **h** for type of sensilla) is divided by the corresponding percentage observed in the full data set (as shown in **e**). A value of 1 for this quotient would indicate that the distributions across the selected KC groups and the full data set are identical. All analyses were also performed on 1,000 shuffled data sets (black circles, ± s.d.). **e**, The glomerular connections in the data set are grouped according to whether they receive input from an OSN that innervates a basiconic (blue), coeloconic (green), trichoid (red) or uncharacterized sensillum (gray). **f-h**, The distribution of the remaining glomerular connections to the 168 KCs receiving at least one input from a basiconic glomerulus, the 104 KCs receiving at least one input from a coeloconic glomerulus, and the 125 KCs receiving at least one input from a trichoid glomerulus are shown.